Molecular Therapy
Nucleic Acids
Original Article

Liver-Targeted Anti-HBV Single-Stranded Oligonucleotides with Locked Nucleic Acid Potently Reduce HBV Gene Expression *In Vivo*

Hassan Javanbakht,[1] Henrik Mueller,[1] Johanna Walther,[1] Xue Zhou,[2] Anaïs Lopez,[1] Thushara Pattupara,[1] Julie Blaising,[2] Lykke Pedersen,[3] Nanna Albæk,[3] Malene Jackerott,[3] Tianlai Shi,[1] Corinne Ploix,[1] Wouter Driessen,[1] Robert Persson,[3] Jacob Ravn,[3] John A.T. Young,[1] and Søren Ottosen[3]

[1]Roche Pharma Research and Early Development, Roche Innovation Center Basel, 4070 Basel, Switzerland; [2]Roche Pharma Research and Early Development, Roche Innovation Center Shanghai, Shanghai 201203, China; [3]Roche Pharma Research and Early Development, Roche Innovation Center Copenhagen, 2970 Hørsholm, Denmark

Chronic hepatitis B infection (CHB) is an area of high unmet medical need. Current standard-of-care therapies only rarely lead to a functional cure, defined as durable hepatitis B surface antigen (HBsAg) loss following treatment. The goal for next generation CHB therapies is to achieve a higher rate of functional cure with finite treatment duration. To address this urgent need, we are developing liver-targeted single-stranded oligonucleotide (SSO) therapeutics for CHB based on the locked nucleic acid (LNA) platform. These LNA-SSOs target hepatitis B virus (HBV) transcripts for RNase-H-mediated degradation. Here, we describe a HBV-specific LNA-SSO that effectively reduces intracellular viral mRNAs and viral antigens (HBsAg and HBeAg) over an extended time period in cultured human hepatoma cell lines that were infected with HBV with mean 50% effective concentration (EC_{50}) values ranging from 1.19 to 1.66 μM. To achieve liver-specific targeting and minimize kidney exposure, this LNA-SSO was conjugated to a cluster of three N-acetylgalactosamine (GalNAc) moieties that direct specific binding to the asialoglycoprotein receptor (ASGPR) expressed specifically on the surface of hepatocytes. The GalNAc-conjugated LNA-SSO showed a strikingly higher level of potency when tested in the AAV-HBV mouse model as compared with its non-conjugated counterpart. Remarkably, higher doses of GalNAc-conjugated LNA-SSO resulted in a rapid and long-lasting reduction of HBsAg to below the detection limit for quantification, i.e., by 3 log10 ($p < 0.0003$). This antiviral effect depended on a close match between the sequences of the LNA-SSO and its HBV target, indicating that the antiviral effect is not due to non-specific oligonucleotide-driven immune activation. These data support the development of LNA-SSO therapeutics for the treatment of CHB infection.

INTRODUCTION

Hepatitis B virus (HBV) infection is a major global health problem. The 8 HBV genotypes (A–H) are geographically distributed worldwide with the major clinical impact coming from genotypes A–D.[1] Despite the availability of successful prophylactic vaccines, the World Health Organization reported in 2016 that more than 250 million people are chronically infected with HBV worldwide[2] Chronic HBV carriers are at risk for developing HBV-related liver complications, such as chronic hepatitis, cirrhosis, and primary hepatocellular carcinoma, during their lifetimes.[3,4]

Hepatitis B surface antigen (HBsAg) loss, also defined as "functional cure," is considered the goal for any new therapy.[5,6] In contrast, currently available standard-of-care treatments for chronic HBV, such as interferon (i.e., polyethylene glycol [PEG]-IFN, also known as Pegasys) and nucleos(t)ide analogs (e.g., tenofovir or entecavir) are associated with low rates of functional cure.[5]

HBV belongs to the *Hepadnaviridae* with a 3.2-kb circular, partially double-stranded DNA genome that establishes persistent infection as a closed covalently circular DNA (cccDNA) in the nucleus of infected hepatocytes.[5,7] The cccDNA encodes seven HBV proteins, which are expressed from five major RNA transcripts, that all share a common 3′ end sequence. The viral genome is replicated through the pregenomic RNA, which in addition to being the template for reverse transcription also acts as the coding mRNA for viral core and polymerase proteins. The precore (pre-C) mRNA is initiated upstream of the pregenomic RNA and serves as template for the production of the hepatitis B e antigen (HBeAg). The 2.4/2.1-kb subgenomic mRNAs code for HBV large-, medium-, and small-envelope (HBsAg) proteins. HBsAg is incorporated into virions and subviral particles that contribute to the virus-specific immune dysfunction, a hallmark

Received 12 August 2017; accepted 18 February 2018;
https://doi.org/10.1016/j.omtn.2018.02.005.

Correspondence: Søren Ottosen, PhD, Roche Pharma Research and Early Development, Roche Innovation Center Copenhagen, F. Hoffmann-La Roche, Ltd., Fremtidsvej 3, Horsholm 2970, Denmark.
E-mail: soren.ottosen@roche.com
Correspondence: John A.T. Young, PhD, Roche Pharma Research and Early Development, Roche Innovation Center Basel, F. Hoffmann-La Roche, Ltd., Grenzacherstrasse 124, Building 68/Room 206, 4070 Basel, Switzerland.
E-mail: john.young.jy3@roche.com

of chronic HBV infection. The 0.75-kb subgenomic mRNA encodes the regulatory protein X (HBx).[7,8]

Chronic infections with HBV advance through multiple phases, including immune tolerant, immune active, inactive carriers, or immune control and reactivation. The immune tolerant phase of the disease in particular is prolonged in duration and is associated with high levels of viremia (circulating HBV DNA), HBeAg, and even higher levels of the non-infectious HBsAg-containing subviral particles.[9] Previous studies suggest that high levels of dominant viral antigens, such as HBsAg in liver and periphery, contribute to the exhaustion or impairment of antiviral $CD8^+$ T cells in chronic HBV infection.[10] Other studies indicate that high level expression of antigens by hepatocytes is associated with a failure to induce multifunctional CD8+ T cell immune responses.[11] HBsAg has also been reported to negatively regulate HBV-specific immune responses by directly modulating immune cell functions,[12–15] and the intrahepatic expression levels of certain innate immunity genes were found to be more down-regulated in CHB patients with higher serum HBsAg levels as compared to CHB patients with lower HBsAg levels.[16,17] Taken together, these studies highlight the potential therapeutic role for agents that selectively reduce both viral loads and antigens as a means to restore immune control of the virus infection.

Oligonucleotide-based gene expression inhibitors are maturing as fully validated therapeutics, with a number of compounds progressing through clinical trials.[18–20] The majority of these are either double-stranded small interfering RNAs (siRNAs), working through the RNA-induced silencing complex (RISC), or relying on a single-stranded-DNA-like molecule, working through an RNase-H-mediated mechanism of mRNA degradation. The current state-of-the art technology for the latter class employs single-stranded oligonucleotides (SSO), comprising a 12- to 20-mer oligonucleotide with phosphorothioate internucleotide linkages, consisting of standard DNA nucleobases throughout the molecule and a mixture of standard ribose residues and modified high-affinity ribose residues, such as ribose with a substitution at the 2′ position or 2′–4′ bicyclic nucleotides. These modifications ensure stability, plasma-protein binding, and target affinity while retaining the ability to direct RNase H activity in the cell.[21]

Unconjugated SSOs naturally accumulate in a number of tissues in the body, with major accumulation in kidney and liver. In fact, accumulation in the kidneys has been shown to be associated with nephrotoxicity in clinical settings.[22,23] Furthermore, although major distribution to the liver is observed, this distribution is not uniform, and unconjugated SSOs preferentially accumulate in non-parenchymal cells. To enhance the activity of SSOs against a hepatocyte-expressed target, preferential SSO delivery to hepatocytes can be achieved through conjugation to a tri-antennary N-acetylgalactosamine cluster (GalNAc) that directs enhanced uptake via the hepatocyte-specific asialoglycoprotein receptor (ASGPR).[24] GalNAc conjugation has made it possible to deliver siRNA into hepatocytes without a need for any additional specific delivery component. As an example, inclisiran ($ALN\text{-}PCS_{SC}$), a GalNAc-conjugated siRNA that targets proprotein convertase subtilisin-kexin type 9 (PCSK9) mRNA, demonstrated remarkable efficacy, durability, and safety in recent clinical investigation.[25] Similarly, previous studies demonstrated that a GalNAc-conjugated SSO targeting apolipoprotein A significantly improved potency over unconjugated SSO *in vivo*.[26] It is expected that the improved potency translates into a significant dose reduction in clinical settings that in turn may result in a more favorable safety profile.

In clinical trials, the furthest advanced RNA therapeutics targeting HBV mRNAs have been siRNAs (ARC 520/521), requiring a complex delivery formulation. ARC 520/521 utilized dynamic poly-conjugates (DPC), a delivery platform developed by Arrowhead pharmaceuticals for the targeted delivery of siRNA to hepatocytes. Whereas ARC520/521 demonstrated proof-of-concept efficacy in preclinical models and clinical trials, the clinical development was discontinued due to toxicity observed in a preclinical study using the DPC delivery platform.[27–29] Other well-described RNA therapeutics in literature include SSOs that required relatively high doses to achieve a marginal potency in mouse models of chronic HBV.[30] In this study, we demonstrate the potency of a locked nucleic acid (LNA)-containing SSO (LNA-SSO) molecule that targets a region of HBV mRNAs common to all viral transcripts. We show that this molecule efficiently reduces viral replication and HBsAg levels in both cultured cells and the adeno-associated virus (AAV)-HBV mouse model of chronic HBV. Furthermore, we demonstrate that conjugation of the LNA-SSO to a cluster of a GalNAc results in an increased uptake in hepatocytes, leading to a long-lasting antiviral effect in the AAV-HBV mouse model.

RESULTS

A Pan-genotypic HBV LNA-SSO that Potently Inhibits HBsAg Production

To identify a potent LNA-SSO inhibitor of HBV replication, we synthesized a library of 13- to 18-mer LNA-SSOs targeting conserved sequences across the viral transcriptome. The *in vitro* antiviral activity of these SSOs was evaluated in the HBV-expressing cell line HepG2.2.15, which expresses viral mRNA and pre-genomic RNA (pgRNA) from HBV DNA sequences integrated into the cellular genome. After treating these cells with LNA-SSO via gymnosis,[31] the levels of HBsAg in the growth medium were measured 6, 9, and 13 days after beginning of treatment (Figure 1A). As expected, SSOs targeting non-overlapping sequences in the pregenomic/precore region had no inhibitory effect on HBsAg levels, as these transcripts do not contribute to HBsAg production (Figure 1B).[7] In contrast, SSOs targeting the regions that encode HBsAg, including where overlapping with the HBx transcript, led to potent inhibition of HBsAg levels. One such potent LNA-SSO, SSO-1, was selected for further characterization based on the following criteria: (1) targeting the 3′ region common to all HBV transcripts (Figure 1B); (2) targeting a sequence in the viral genome that is highly conserved between major HBV genotypes (A–D) with >95% coverage of all available complete genome sequences in the NCBI database (Figure 1C)

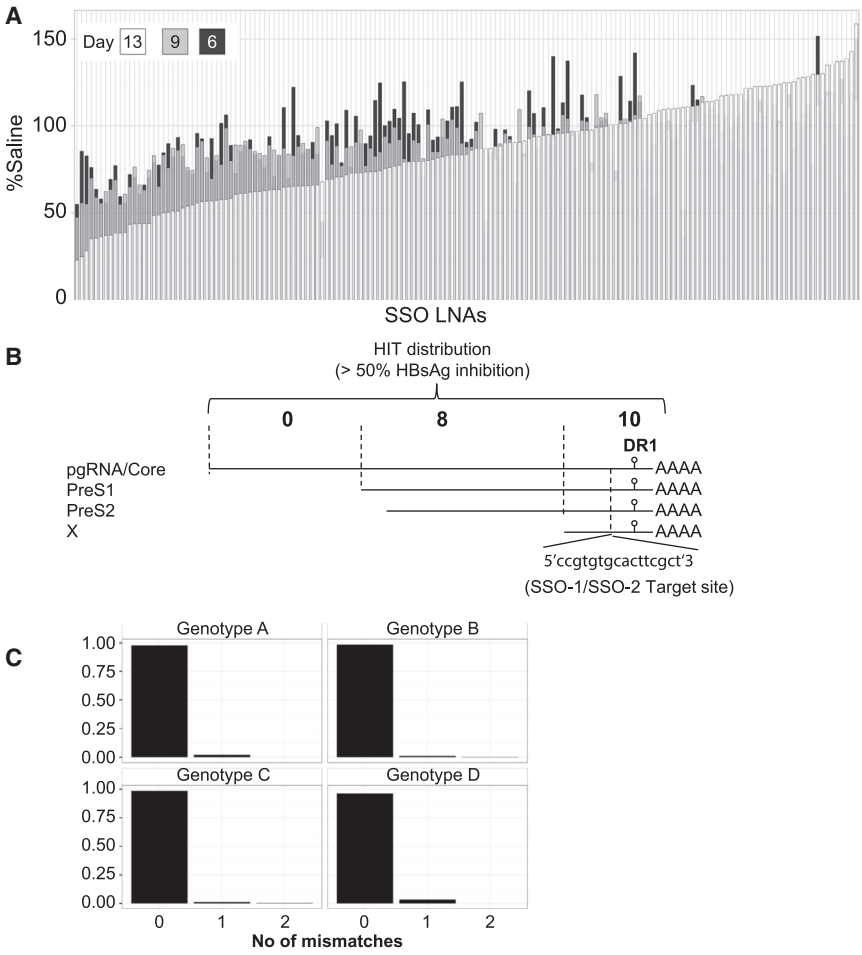

Figure 1. Discovery of SSO-1 and SSO-2

(A) LNA-SSOs targeted to both HBsAg and HBx region can mediate effective inhibition of HBsAg expression in HepG2.2.15 cells. HepG2.2.15 was treated with a series of HBV-targeting unconjugated LNA-SSOs (HBV LNA) of gapmer design at 25 μM by simple addition to the growth medium and assayed for HBsAg expression by CLIA on days 6, 9, and 13. A single representative dataset is presented. The compounds are arranged by their anti-HBsAg potency. (B) Distribution of target sites for LNA-SSOs that exhibited more than 50% of HBsAg inhibition with respect to HBV mRNAs is shown. SSO-1 target sequence 1,575–1,591 with reference to NC_003977.2 NCBI HBV genome is also shown. (C) The SSO-1 target site is conserved within the major viral genotypes A, B, C, and D, with greater than 95% of unique sequences having no mismatches (0MM) and the balance having a single mismatch to the oligo (1MM). Only very few instances of 2 mismatches (2MM) or more (not shown) to the four major genotypes were observed.

within genotypes or across genotypes A–H (data not shown); and (3) targeting no other sequence in human or mouse transcriptomes (Figure S1).

GalNAc Conjugation of LNA-SSO Improves Anti-HBV Potency of SSO-1 in Cultured Hepatoma Cells

As demonstrated previously, the GalNAc sugar moiety can redirect RNA therapeutics to hepatocytes[26,32] through interaction with the hepatocyte-specific ASGPRs, thus improving functional uptake of the active oligonucleotide to the hepatocyte. Seeking to take advantage of this mechanism, a GalNAc-conjugated derivative of SSO-1 (SSO-2) was designed, comprising a cluster of three GalNAc moieties, linked to the 5′ end of the SSO-1 (Figure 2A). A non-complementary dinucleotide linker with a labile phosphodiester backbone was inserted to bridge the LNA-SSO and the GalNAc cluster.

SSO-1 and SSO-2 were tested for their relative potencies in a differentiated human hepatoma cell line HepaRG (dHepaRG).[33] This cell line expresses low levels of ASGPR; therefore, the compound's antiviral activity was also measured in dHepaRG ASGPR1/2 cells that were engineered to overexpress the ASGPR1/2 receptors. Confirmation of the expression levels of ASGPR in this cell line was achieved using both western blot and fluorescence-activated cell sorting (FACS) analysis (Figures 2B and 2C). After infection with HBV, these cell lines were exposed to increasing doses of SSO-1, SSO-2, or a GalNAc-conjugated negative control LNA-SSO (SSO-3). Intracellular (mRNA) and extracellular viral markers (HBsAg and HBeAg) were evaluated after 7 days of the LNA-SSO treatments (Figures 3A and 3B), and the EC_{50} for the inhibition of each viral marker was determined (Figure 3C). As expected, SSO-1 demonstrated equal potency in both dHepaRG and dHepaRG-ASGPR1/2-infected cells as judged by measuring HBsAg, HBeAg, and HBV mRNA levels. By contrast, the GalNAc-conjugated SSO-2 was 5- to 8-fold more potent in the dHepaRG ASGPR1/2-infected cells than in the parent dHepaRG cell line. The negative control LNA-SSO, SSO-3, had no antiviral effect in either cell line. Taken together, these data demonstrated the potential of the GalNAc-conjugated LNA-SSO for efficient knockdown of viral gene expression in infected hepatocyte-like cells that express ASGPR.

GalNAc Conjugation Improves Antiviral Effect of an HBV LNA-SSO *In Vivo*

The *in vivo* efficacy of the GalNAc-conjugated LNA-SSO, SSO-2, was tested in the AAV-HBV mouse model.[34,35] Chronic infection of mouse hepatocytes with a recombinant AAV-HBV virus was established in this model, and the animals were then treated with SSO-1, SSO-2, or with the HBV polymerase inhibitor entecavir as a control.

Animals were dosed twice weekly with 0.038, 0.19, and 0.94 μmol/kg of the unconjugated SSO-1 (Figure 4A) or the GalNAc-conjugated SSO-2 (Figure 4B) by subcutaneous injection on days 0, 3, 6, and 9

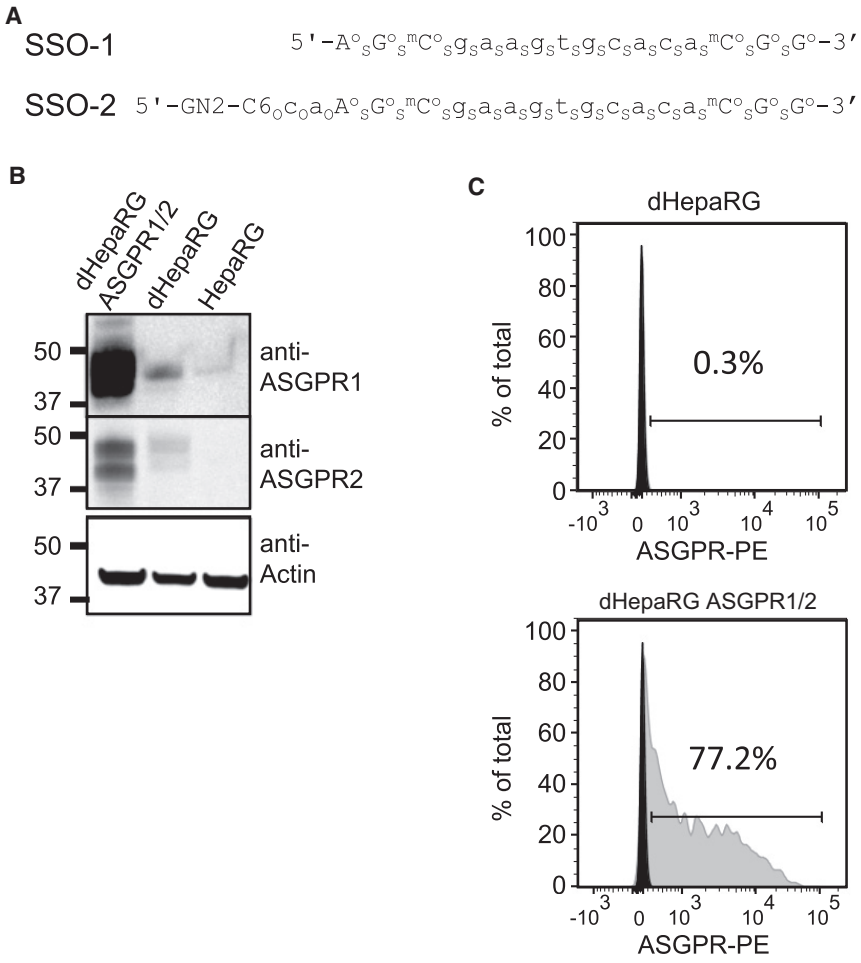

Figure 2. GalNAc-Conjugated LNA-SSO and Protein and Surface Expression of ASGPR Receptor

(A) SSO-1 and SSO-2 are unconjugated and GalNAc-conjugated LNA-SSOs, respectively, containing the same active HBV-directed gapmer sequence. Sequence and structure: uppercase letters with superscript O, oxy-LNA; lower case letters, DNA; subscript S, internucleoside phosphorothioate bond; subscript O, internucleoside phosphodiester bond; superscript m, methyl-cytosine; GN2-C6, tri-antennary GalNAc cluster. (B) ASGPR protein levels of HepaRG overexpressing ASGPR-1/-2 was assessed by western blotting and compared to differentiated (dHepaRG) and undifferentiated HepaRG (HepaRG). Anti-actin Ab was used as loading control. (C) Surface expression of ASGPR-1 (gray) on dHepaRG and dHepaRG ASGPR1/2 was assessed by FACS analysis and compared to isotype control (black).

(a total of 4 doses). Circulating HBsAg, HBeAg, and HBV DNA levels were monitored twice weekly during dosing and for two weeks after the last dose was administered. The reduction in circulating viral parameters at day 16 is represented in the table in Figure 4C for both SSO-1 and SSO-2.

Treatment with the unconjugated compound SSO-1 at 0.94 μmol/kg resulted in a limited, dose-dependent reduction in the HBsAg levels (Figure 4A). Whereas there was a clear reduction in all viral parameters at this high dose, there was no convincing effect on these parameters by the lower doses of 0.038 and 0.19 μmol/kg. Furthermore, the durability of the antiviral response was limited and the effect on all three markers was seen to be diminished at day 24 at all doses. These data are highly consistent with a previous report demonstrating only high doses of 30 mg/kg of unconjugated SSO reduced viral parameters by 2 $\log_{10}$.[30]

In contrast, SSO-2 treatment led to a rapid and dose-dependent reduction of all virus markers after the first viral readout on day 3, with the exception that HBV DNA levels achieved at the mid and top doses appeared to have a saturated response at early time points. A rapid and long-lasting reduction of HBsAg below the detection limit for quantification, i.e., by at least 3 $\log_{10}$ ($p < 0.0003$), was observed for the 0.94 μmol/kg dose of SSO-2 (Figure 4B). Furthermore, the duration of the effect for all doses was beyond the duration of the study for all viral markers, in particular for the high-dose group, where no rebound of viral markers was observed during the two weeks off-treatment period.

Confirming the durability of response to SSO-2, intracellular HBV core levels in mouse livers treated with SSO-2 at 0.94 μmol/kg were evaluated at the end of off-treatment period (Figure 5). The immunohistochemistry analysis confirmed a remarkable and durable reduction of intrahepatic HBV core protein levels for SSO-2 high-dose-treated group compared to control group.

Furthermore, the effect of the GalNAc-conjugated LNA-SSO on viral gene expression is clearly differentiated from standard-of-care (entecavir) therapy, which resulted in reduced HBV DNA, but not reduced HBsAg levels, in this model system (Figure S2).

Taken together, GalNAc conjugation of anti-HBV LNA-SSO leads to a potent, long-lasting antiviral effect with clear improvement over a non-liver-targeted LNA-SSO.

GalNAc Conjugation of LNA-SSO Leads to Preferential Liver Targeting

We reasoned that the increased efficacy seen with the GalNAc-conjugated versus non-conjugated LNA-SSO was most likely due to the specific delivery of this molecule to hepatocytes and consequently reduced exposure to other organs. The change in distribution between liver and kidney was confirmed by dosing mice with a single 0.18 and 0.94 μmol/kg dose of SSO-1 or SSO-2 followed by sacrifice at 48, 96,

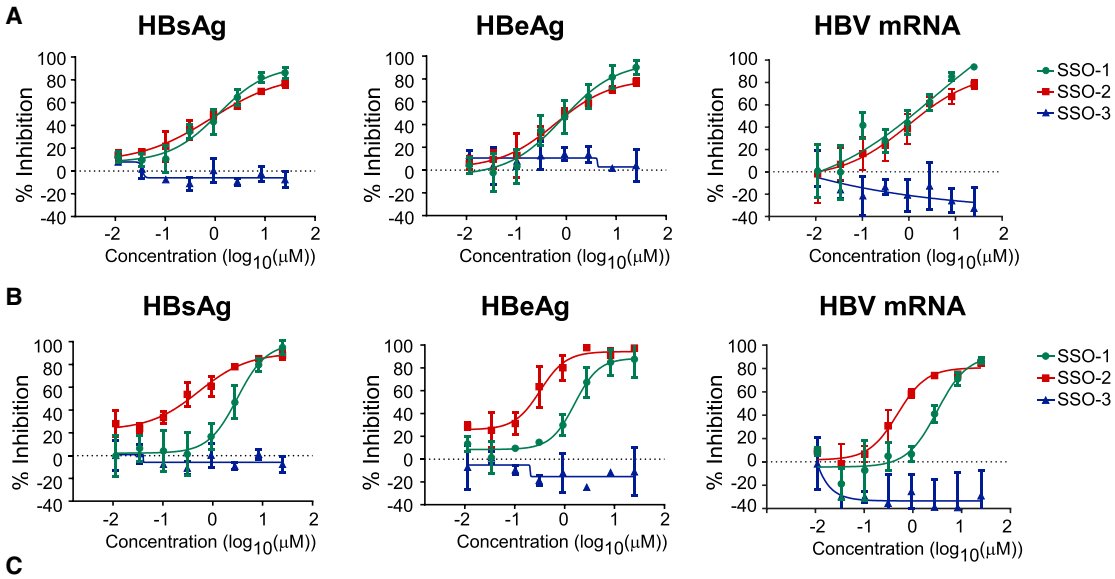

C

Cell line Tested	Test compounds	HBsAg		HBeAg		Intracellular HBV mRNAs	
		EC_{50} (μM)	SD*	EC_{50}(μM)	SD*	EC_{50} (μM)	SD*
dHepaRG cell line	SSO-1	1.19	0.23	1.24	0.56	1.66	0.78
	SSO-2	0.91	0.25	0.86	0.22	2.45	0.77
	SSO-3	> 25	n/a	> 25	n/a	> 25	n/a
dHepaRG ASGPR 1/2 cell line	SSO-1	3.40	0.52	2.58	2.56	3.45	0.37
	SSO-2	0.41	0.10	0.35	0.03	0.40	0.07
	SSO-3	> 25	n/a	> 25	n/a	> 25	n/a

n/a: Not applicable
*Standard deviation (n=3)
No significant cytotoxicity observed in any groups up to 25 μM, the highest concentration tested

Figure 3. Overexpression of ASGPR-1/-2 Increases Antiviral Activity of Anti-HBV LNA-SSO upon GalNAc Conjugation
(A and B) Inhibition of HBsAg and HBeAg secretion and intracellular mRNA levels in HBV-infected dHepaRG-WT (A) and dHepaRG-ASGPR-1/-2 (B) cells after treatment with anti-HBV LNA-SSO (SSO-1), GalNAc-conjugated anti-HBV LNA-SSO (SSO-2), and control LNA-SSO (SSO-3). Error bars, SD (n = 3). (C) Table represents the average EC_{50} values for all measured anti-HBV markers in both cell lines of three independent experiments.

and 192 hr. Liver and kidneys were harvested and assayed by a hybridization ELISA assay to measure LNA-SSO distribution. These experiments revealed that the uptake of SSO-2 was five-fold higher in the liver than in the kidney (Figure 6A). Conversely, concentration of unconjugated SSO-1 was three-fold higher in the kidney than in the liver. It should be noted that the change in liver/kidney distribution for SSO-2 is less pronounced at higher dose levels. The dose levels used in this study are near the predicted saturation level of the receptor (ASGPR), and it is likely that the higher dose exceeds saturation, resulting in proportionally lower uptake to the liver.[36]

In situ hybridization analysis of SSO-1 and -2 confirmed that the presence of the GalNAc moiety affected cellular distribution of the SSO (Figure 6): the unconjugated LNA-SSO was observed to mainly accumulate in a minor subset of small, most likely non-parenchymal cells, whereas the GalNAc-conjugated LNA-SSO was broadly distributed throughout the liver, with reduced accumulation in the presumed non-parenchymal cells and increased accumulation in larger, more numerous cells (Figure 6B). These larger cells are morphologically consistent with hepatocytes. Therefore, these data demonstrate that the increase in the potency of the GalNAc conjugated correlates with a change in the distribution of the SSO to include most cell types in liver, likely including the hepatocytes.

In Vivo Antiviral Activity Is Target Sequence Dependent

A possible concern of oligonucleotide-based antiviral therapies is that their efficacy may be impacted by host-pattern-recognition-receptor-mediated innate immune-signaling pathways reacting to free nucleotide.[37,38] In order to evaluate the likelihood of such pathways being involved in the activity of SSO-2, two derivative compounds, SSO-4 and SSO-5, were generated carrying one or two sequence mismatches to the viral target, respectively (Figure 7). Consistent with a sequence-specific efficacy for SSO-2, the two derivative molecules had markedly reduced antiviral activity in the dHepaRG ASGPR1/2 cell culture system described above (Figures 7A and 7B). These compounds were also tested in the AAV-HBV mouse model, where they were dosed twice weekly at 0.19 μmol/kg for two weeks and then monitored for an additional two weeks during the off-treatment period. By contrast to SSO-2, which reduced HBsAg levels by 2.0 $\log_{10}$ ($p < 0.0001$) at day 16 post-treatment, SSO-4 only reduced HBsAg levels by 1.22 $\log_{10}$

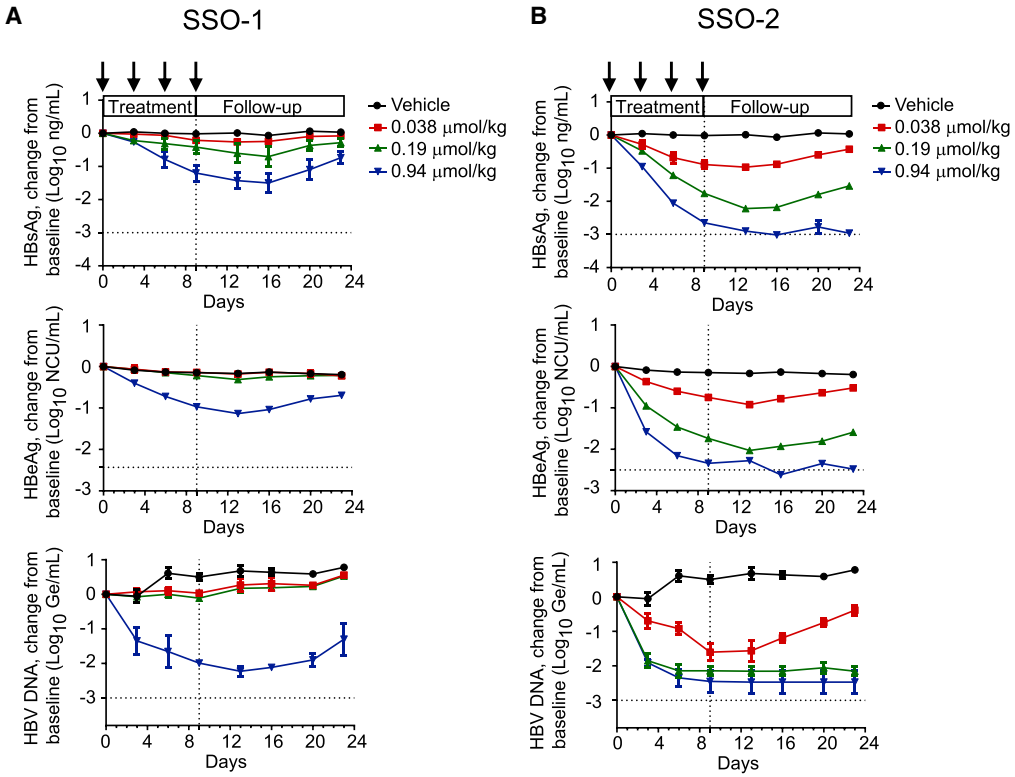

C

Test compounds	Dose level (µmol/kg)	HBsAg			HBeAg			HBV DNA		
		Day 16 #	SEM ^	ρ*	Day 16 #	SEM ^	ρ*	Day 16 #	SEM ^	ρ*
Saline	n/a	-0.07	0.08	0.43	-0.14	0.03	0.003	0.64	0.24	0.04
SSO-1	0.038	-0.43	0.21	0.11	-0.14	0.10	0.21	0.31	0.53	0.59
SSO-1	0.19	-0.25	0.08	0.02	-0.25	0.04	0.0014	0.19	0.12	0.17
SSO-1	0.94	-1.50	0.31	0.003	-1.04	0.03	< 0.0001	-2.12	0.19	< 0.0001
SSO-2	0.038	-0.88	0.24	0.01	-0.78	0.03	< 0.0001	-1.19	0.27	0.004
SSO-2	0.19	-2.18	0.08	< 0.0001	-1.93	0.02	< 0.0001	-2.16	0.13	< 0.0001
SSO-2	0.94	-3.02	0.05	< 0.0001	-2.62	0.04	< 0.0001	-2.47	0.33	0.0003

#: Log change from the pre-treatment (Day 0) value

^: Standard error of the mean (n=4)

*: Student's *t*-test by GraphPad Prism 6

n/a: Not applicable

Figure 4. Effect of SSO-1 and SSO-2 on HBV Viral Markers in Serum from AAV-HBV-Infected Mice

AAV-HBV mice were treated with saline (control), SSO-1, or SSO-2 at the indicated dose levels on days 0, 3, 6, and 9. (A and B) Serum HBsAg, HBeAg, and HBV DNA levels were determined during the treatment and follow-up period for SSO-1 (A) and SSO-2 (B) compared to the vehicle control. Error bars, SEM (n = 4). (C) The reduction in circulating viral parameters at day 16 (one week after treatment was stopped) is summarized in a table. Dose levels of 0.038, 0.19, and 0.94 µmol/kg correspond to 0.20, 1.0, and 5.0 mg/kg for SSO-1 and 0.28, 1.4, and 7.0 mg/kg for SSO-2, respectively.

(p = 0.0009), and SSO-5 had no significant effect on HBsAg levels (Figures 7C and 7D).

Moreover, when examining the antiviral SSOs in a whole blood assay against pattern recognition receptor agonists, poly(dG:dC), CpG, or R848, neither the naked nor conjugated SSO triggered a cytokine response (Figure 8). And neither LNA-SSO-1 nor SSO-2 had an effect on complement activation when compared to alternative and classic pathway complement activators (Figure 8). In addition, a generalized hepatotoxic mode of action for these compounds could be dismissed, as neither SSO-1 nor SSO-2 modulated the alanine aminotransferase (ALT) serum levels (a marker of hepatotoxicity) in treated mice compared to vehicle control (Figure S3).

These data support that the SSO-1 and SSO-2 antiviral activity is driven by target affinity and thus RNase-H-mediated target degradation and not due to triggering a host innate immune response or a generalized hepatotoxic response.

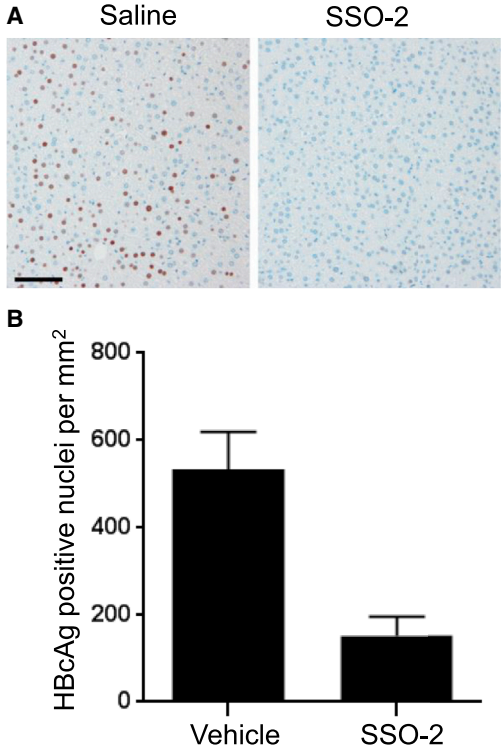

Figure 5. Quantification of HBcAg-Positive Cells in Liver of AAV-HBV-Infected Mice

(A) Immunohistochemical staining for HBcAg (labeled dark brown) in liver sections from AAV-HBV-transduced mice treated with vehicle or with SSO-2 (0.94 μmol/kg) at the end of off-treatment period. Bar represents 100 μm. (B) HBcAg-positive cells were detected using image analysis and expressed in % of the area of the tissue section. Non-parametric statistical analysis showed significantly reduced number of HBcAg-positive cells per area in mice treated with HBV LNA compared to vehicle group ($p < 0.01$). Dose level of 0.94 μmol/kg corresponds to 7 mg/kg of SSO-2. Error bars, SD (n = 6).

DISCUSSION

Current standard-of-care nucleos(t)ide analogs act by inhibition of HBV polymerase activity, resulting in decrease of viral replication and viral load. Therefore, they do not affect HBV gene expression and viral antigen production in infected hepatocytes. Next-generation therapies for chronic HBV infection seek to achieve higher levels of functional cure as defined by durable loss of HBsAg, a viral marker that is negatively correlated with good clinical outcome. With this goal in mind, several groups, including our own, are developing oligonucleotide therapeutics, which are potent inhibitors of HBV gene expression. Here, we have described the potent activity associated with a GalNAc-conjugated LNA-SSO that targets all 5 major viral RNA transcripts and that was associated with preferential exposure to the liver as opposed to the kidney. This LNA-SSO demonstrated superior antiviral efficacy as compared to its unconjugated counterpart, as judged by HBsAg reduction both in natural infection assay, in which both HBV replication and expression are driven by viral cccDNA, and in the AAV-HBV mouse model, where HBV expression originates from both episomal AAV-HBV vector and HBV cccDNA.[39] Most importantly, the effect of this oligonucleotide was highly dependent upon an exact sequence match to its target viral RNA sequence, and it was not associated with non-specific cytokine, complement, or other generalized toxicity induction.

There are a number of advantages of directly targeting viral RNA with an HBV therapeutic. First, virally expressed transcripts are unique and distinguishable from the host transcripts based on their nucleotide sequence content. Second, HBV has relatively low mutation rate, compared to other therapeutically relevant viral species. This means certain sequences in viral RNA transcripts that are highly conserved between different HBV genotypes and subtypes making it possible to design pan-genotypic therapeutics. Third, all HBV viral transcripts, including those (2.4-kb/2.1-kb RNAs) that code for HBsAg, all share a common 3′ end (Figure 1B), and therefore, it is also possible to design an oligonucleotide therapeutic that eliminates the expression of all viral proteins. This would allow a single therapeutic agent to overcome any potential for host immune suppression that has been associated with each of the major viral proteins.[16,17,40–42] Finally, because HBV is a hepatotropic virus that replicates exclusively in hepatocytes, engineering the oligonucleotide to specifically target hepatocytes through ASGPR-mediated uptake, using GalNAc-derivatives of the oligonucleotide drug reduces exposure in irrelevant tissues while maximizing the antiviral effect.[43,44]

Impaired HBV-specific immune responses and establishment of persistent viral cccDNA are thought to be the essential components for the chronicity of HBV infection.[45] Because the viral cccDNA has a very low turnover, we do not expect that transient reduction of viral transcripts associated with a short duration treatment course by LNA-SSO alone is sufficient to impact the size of the cccDNA pools significantly.[46] However, the combination of the LNA-SSO-mediated therapy with other antivirals directly targeting the replication would potentially affect cccDNA levels significantly with possible elimination of the cccDNA pools over a finite treatment period. Furthermore, previous studies suggest that the high levels of antigen expression in liver impair both the innate and adaptive antiviral immune responses in the chronic infection.[11,17,47] Therefore, we expect that the direct reduction of expression of all viral antigens using LNA-SSO, when combined with immunomodulators, would aid to re-establish the virus-specific immune response. We anticipate that combinations of the gene expression inhibitors, such as the LNA-SSO described in this paper, with both replication inhibitors and immune enhancers are likely to be the key to achieve the functional cure.

Currently, there are two liver-targeted RNA therapeutics in clinical development for treatment of chronic HBV.[48] ALN-HBV is a GalNAc-conjugated siRNA that targets the conserved region of HBV genome. A phase 1/2 clinical trial of ALN-HBV was initiated in July 2016. However, Alnylam Pharmaceuticals discontinued the development of ALN-HBV01 to advance a new development candidate, ALN-HBV02, that employs Enhanced Stabilization Chemistry-Plus (ESC+) GalNAc conjugate technology.[49] GSK-3389404 (IONIS-HBV-LRx) is a GalNAc-conjugated SSO that is currently in

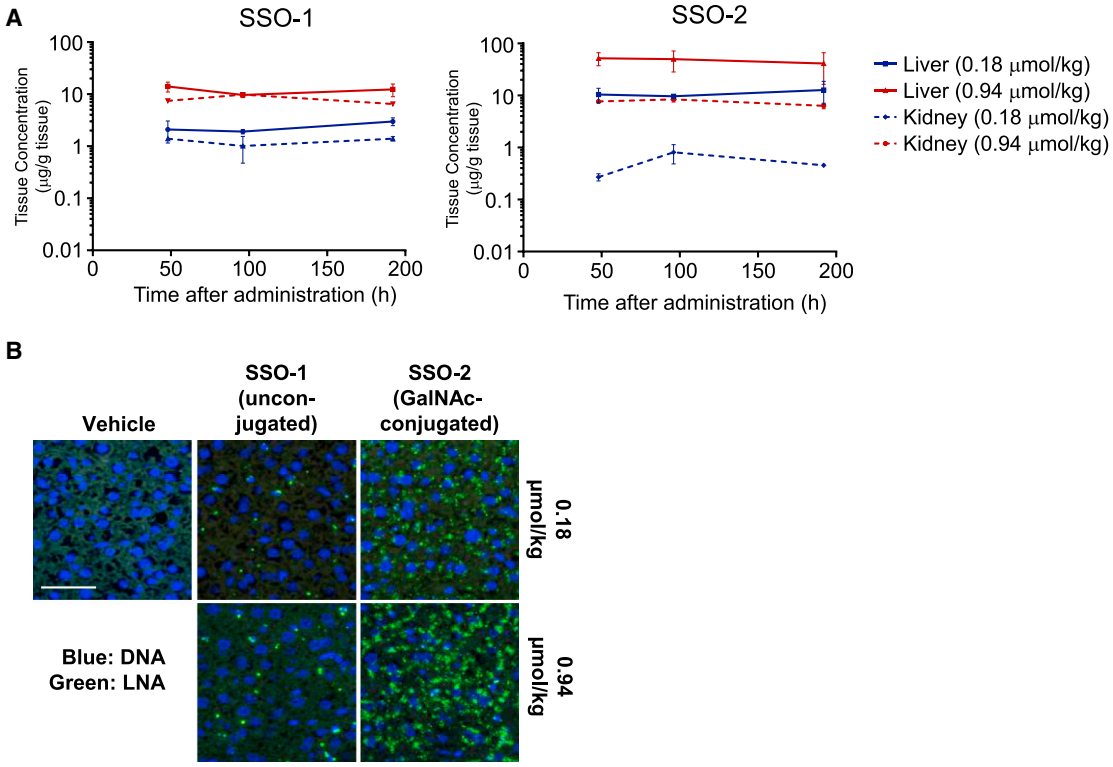

Figure 6. The GalNAc-Conjugated SSO Is Preferentially Delivered to the Liver

C57BL/6 mice were administered with SSO-1 and corresponding conjugated SSO-2 as a single dose of 0.18 and 0.94 μmol/kg (2 animals per dose level and compound). (A) At different times after dosing (up to 184 hr), liver and kidney samples were prepared and the oligonucleotide concentration determined by hybridization-ELISA in the samples. Error bars, SD (n = 2). (B) At 24 hr, mice treated with SSO-1 and SSO-2 at 0.18 and 0.94 μmol/kg or treated with vehicle were sacrificed and the liver SSO concentration and localization visualized via *in situ* hybridization. SSO-1 and SSO-2 were visualized using standard *in situ* methods using the same FAM-labeled LNA-SSO-containing-oligonucleotide with full complementarity to both molecules. Bar represents 100 μm. Dose levels of 0.18 and 0.94 μmol/kg correspond to 1.0 and 5.0 mg/kg for SSO-1 and 1.4 and 7.0 mg/kg for SSO-2, respectively.

clinical development. Because the structure and target sequences of ALN-HBV1/2 and GSK-3389404 have not yet been disclosed, it was not possible for us to make any substantial comparable studies between liver-targeted LNA-SSOs and ALN-HBV02 or GSK-3389404.

The LNA platform has already been clinically validated for antiviral potential through the development of miravirsen, a microRNA (miRNA) that blocks HCV replication.[50] This increases confidence in this therapeutic mode of action for the treatment of CHB. Future preclinical studies with this and other liver-targeted anti-HBV LNA-SSO molecules will be aimed at exploring the possibility of this technology to induce durable HBsAg loss either when administered as a monotherapy or in combination with other antivirals and immunomodulatory molecules.

MATERIALS AND METHODS

Synthesis of LNA-SSO

Single-stranded LNA oligonucleotides SSO-1–5 (Figures 2A, 7A, and 7B) were synthesized using standard phosphoramidite chemistry. Upper case denotes LNA, lower case DNA. Subscripts S and O denote phosphorthioate and phosphordiester linkages, respectively. DNA phosphoramidites were purchased from Sigma-Aldrich (St. Louis, MO), and LNA phosphoramidites were produced in house (LNA oligonucleotides are also commercially available from QIAGEN [Hilden, Germany]). Aminolinker C6 was purchased from Link Technologies (Bellshill, Scotland).

Unconjugated SSO-1 and 5′-aminolinker C6 precursors (for SSO-2–5) were synthesized on NittoPhase HL UnyLinker 350 support (Kinovate, Oceanside, CA) on an ÄKTA Oligopilot (GE Healthcare, Brondby, Denmark) at 130 μmol scale. After synthesis, the oligonucleotides were cleaved from the support using aqueous ammonia at 65°C overnight. The oligonucleotides were purified by ion exchange on SuperQ-5PW gel (Tosoh Bioscience, Griesheim, Germany) and desalted using a Millipore membrane. After lyophilization, the SSOs were finally characterized by liquid chromatography-mass spectrometry (reverse phase and electrospray ionization-mass spectrometry).

GalNAc-conjugated SSO-2–4 were prepared using GalNAc cluster (GN2) as described in patent application WO 2017/021385 A1 (examples 1–10).[51] The free GalNAc acid was activated using

A

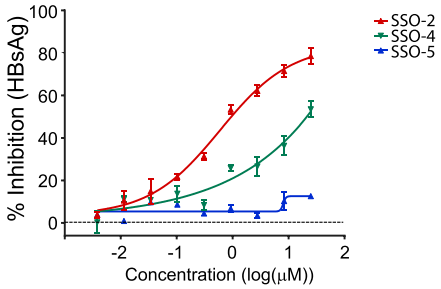

B

Test compounds	HBsAg		Cytotoxicity
	EC_{50} (μM)	SD*	CC_{50} (μM)
SSO-2	0.68	0.08	> 25
SSO-4	>25	n/a	> 25
SSO-5	>25	n/a	>25

*Standard deviation (n=4)

n/a: Not applicable

SSO-2: 5'-GN2-C6caAGCgaagtgcacaCGG
SSO-3: 5'-GN2-C6caAGCgaagtgcagaCGG
SSO-4: 5'-GN2-C6caAGCgcagtgaacaCGG

C

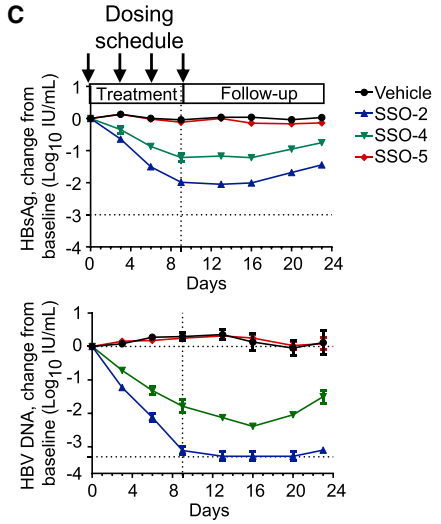

D

Test compounds	Dose level (μmol/kg)	HBsAg			HBV DNA		
		Day 16 #	SEM ^	ρ*	Day 16 #	SEM ^	ρ*
Saline	n/a	0.09	0.10	0.40	0.13	0.27	0.66
SSO-2	0.19	-2.01	0.05	< 0.0001	-3.28	0.13	< 0.0001
SSO-4	0.19	-1.22	0.20	0.0009	-2.39	0.32	0.0003
SSO-5	0.19	-0.14	0.08	0.14	0.25	0.15	0.14

#: Log change from the pre-treatment (Day 0) value

^: Standard error of the mean (n=4)

*: Student's *t*-test by GraphPad Prism 6

n/a: Not applicable

Figure 7. The GalNAc-Conjugated SSO-2 Antiviral Activity Is Target Sequence Dependent

(A) Inhibition of HBsAg secretion was measured by CLIA from supernatant of HBV-infected dHepaRG ASGPR1/2 after treatment with GalNAc-conjugated HBV LNA-SSO as SSO-2 and its variants harboring either one or two mismatches, SSO-4 and SSO-5, respectively. Error bars, SD (n = 3). (B) Table represents the average EC_{50} values for inhibition of HBsAg production from three independent experiments. (C) AAV-HBV mice were treated with saline (control), SSO-2, SSO-4, or SSO-4 at 0.18 μmol/kg on days 0, 3, 6, and 9. Serum HBsAg was determined during the treatment and follow-up period. Error bars, SEM (n = 4). (D) The reduction in circulating HBsAg and HBV DNA at day 16 (one week after treatment was stopped) is summarized in a table. Dose level of 0.18 μmol/kg corresponds to 1.4 mg/kg of SSO-2, SSO-4, and SSO-5.

N-hydroxysuccinimide and *N*-(3-dimethylaminopropyl)-*N*′-ethyl-carbodiimide hydrochloride (EDC) in a mixture of dimethylformamide (DMF) and DMSO and then added to the 5′-aminolinker C6 precursor (3 or 4 molar excess of GN2) in 20 mM aqueous sodium hydrogen carbonate together with triethylamine. After 5–16 hr, the reaction mixture was applied directly to ion-exchange purification and desalting as described for unconjugated SSO.

HepG2.2.15 Assay

HepG2.2.15 cells were cultured in DMEM+GlutaMAX I (Gibco; no. 31966-021) supplemented with 10% HI FBS (Gibco; no. 10082147), 0.23 mg/mL Geneticin (Gibco; no. 10131-027), and 1× penicillin (pen)/streptomycin (strep) (Gibco; no. 15140-122).

The cells were trypsinized, seeded out into white 96-well plates at 5K cells per well, and treated with the HBV LNA-SSO compounds on day 0. Treatments were done at a final concentration of 25 μM with triplicates for each compound. As positive control, a dilution series of a small molecule known to inhibit HBsAg production in HepG2.2.15 was used. On days 6 and 9, the supernatant was harvested to measure secreted HBsAg using the HBsAg CLIA kit (Chemiluminescence Immunoassay; Autobio Diagnostic; no. CL0310-2), the medium on the cells renewed, and fresh compound added. On day 13, the experiment was ended, the supernatants were used for HBsAg determination, and the cell viability was tested.

For the CLIA, supernatants (50 μL/well) and enzyme conjugates (50 μL/well) were transferred into the CLIA plate. After incubating at room temperature (RT) on a shaker for 1 hr, the plates were washed with 1× PBS-T and 25 μl/well of both substrate A and substrate B were added. After shaking at RT on a shaker for 10 min, the luminescence was read on an Envision luminometer with an integration time of 0.2 s. Percentages of HBsAg secretion were calculated by comparing the relative HBsAg secretion in the LNA-SSO-treated

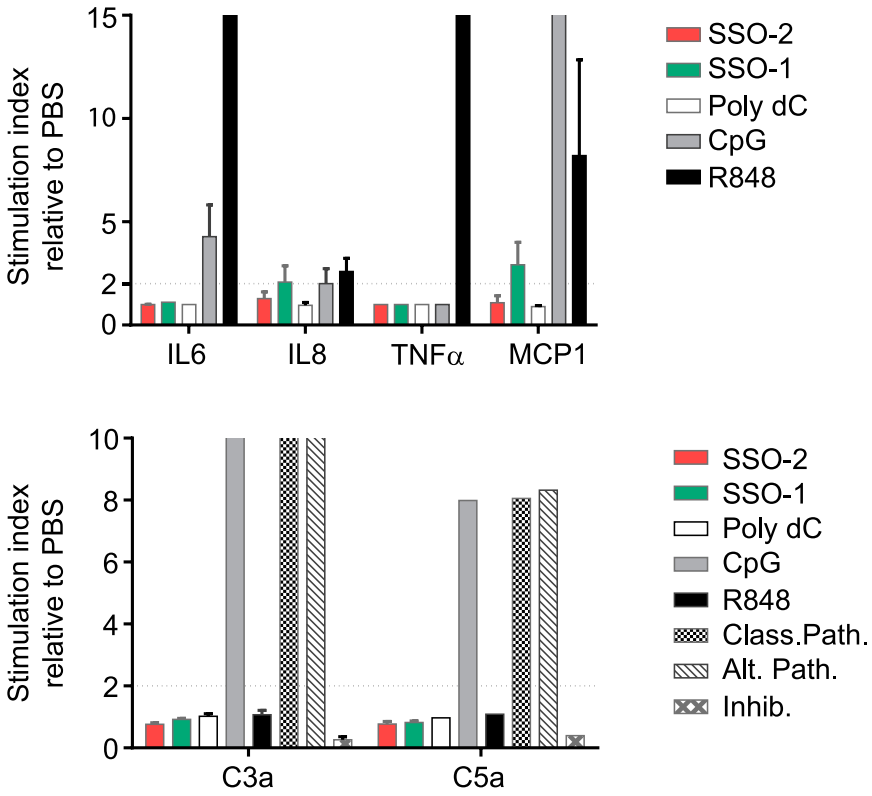

Figure 8. *In Vitro* Immunotoxicity Screening Assay
Oligonucleotides and controls were incubated in freshly drawn blood from 3 healthy human donors. Complement biomarkers C3a and C5a and the cytokine biomarkers interleukin-6 (IL-6), IL-8, tumor necrosis factor alpha (TNF-α), and monocyte chemoattractant protein-1 (MCP1) were measured at 45 min and 6 hr and reported as stimulation index (SI) over PBS. A mean SI increase above 2-fold was considered indicative of potential *in vivo* immunotoxicity of the oligonucleotide. Zymosan and heat-aggregated IgG were used as alternative pathway (Alt. Path.) and classical pathway (Class. Path.) activators, respectively. Inhibitor (Inhibit.), a specimen stabilizing solution, was used as a negative control in these experiments. Error bars, SD (n = 3).

samples with that measured in the untreated "no drug" control (NDC) samples.

The cell viability was tested by adding 80 µl/well CellTiter-Glo One Solution Assay Reagent (Promega; no. G8462) to the cells, shaking the plate at RT for 10 min, and then reading the luminescence on an Envision luminometer using an integration time of 0.2 s. Percentages were calculated by comparing the relative ATP concentration in the LNA-SSO-treated samples with that measured in the NDC samples.

DHepaRG/dHepaRG ASGPR1/2 HBV Infection Assay

HepaRG cells (Biopredic International, Saint-Gregoire, France) were cultured in Williams E Medium+GlutaMAX-I supplemented with 10% HepaRG Growth supplement (cat no. ADD711C Biopredic) and 1× pen/strep (Gibco) and differentiated using 1.8% DMSO for at least 4 weeks before infection. HepaRG ASGPR1/2 cells were generated using a lentiviral method. Proliferating HepaRG cells were transduced at MOI 300 with a lentivirus produced on demand by Sirion Biotech (CLV-CMV-ASGPR1-T2a_ASGPR2-IRES-Puro) coding for Human ASGPR1 and 2 under the control of a CMV promoter and a puromycin resistance gene. Transduced cells were selected for 11 days with 1 µg/mL puromycin and then maintained in the same concentration of antibiotic to ensure stable expression of the transgenes. HBV genotype D was derived from HepG2.2.15 cell culture supernatant and was concentrated using PEG precipitation. To evaluate activity of test compounds against HBV, differentiated HepaRG (dHepaRG) and HepaRG ASGPR1/2 (dHepaRG ASGPR1/2) cells in 96-well plates were infected with HBV at an MOI of 20–30 for 20 hr before the cells were washed 4 times with PBS to remove the HBV inoculum. At day 4 post-infection, cells were treated with different concentrations of the test compounds. Medium was changed with new test compound at day 7 post-infection. Supernatants and cells were harvested and used for HBV marker analysis on day 11 post-infection. Cytotoxicity of test compounds was evaluated in HBV-infected cells using CellTiter-Glo Luminescent Cell Viability Assay (Promega) according to the manufacturer's protocol.

HBV DNA was extracted from the cell culture supernatant using a MagNA Pure 96 robot and the MagNA Pure 96 DNA and Viral Nucleic Acid Small Volume Kit (Roche) according to the manufacturer's protocol. Quantification of HBV DNA was performed in duplicates using a QuantStudio 12K Flex (Life Technologies), the TaqMan Gene Expression Master Mix (Applied Biosystems), and the following primers and probe (IDT): forward core primer (CTGTGCCTTGGGTGGCTTT); reverse core primer (AAGGAAAGAAGTCAGAAGGCAAAA); and probe (56-FAM/AGCTCCAAA/ZEN/TTCTTTATAAGGGTCGATGTCCATG/3IABkFQ). The qPCR was performed using the following settings: uracil-DNA glycosylase (UDG) incubation (2 min; 50°C); enzyme activation (10 min; 95°C); and qPCR (40 cycles with 15 s; 95° for denaturing and 1 min; 60°C for annealing and extension). DNA copy numbers were calculated from Ct values based on a HBV plasmid DNA standard curve by the QuantStudio software.

DNA copy numbers and HBsAg and HBeAg relative luciferase units (RLUs) were used to generate dose-response curves and to calculate EC_{50} values using Prism 6 (GraphPad Software). Values were normalized to the cell control (uninfected cells) and the no drug control (infected but untreated cells). Cell viability data were

normalized to the "no cell" control (medium without cells) and no drug control.

Intracellular HBV mRNA was extracted from cells using a MagNA Pure 96 robot and the MagNA Pure 96 Cellular RNA Large Volume Kit (Roche) according to the manufacturer's protocol. cDNA synthesis was performed from total RNA using the SuperScript III First Strand Synthesis kit (Invitrogen). HBV cDNA was quantified in duplicates by qPCR using a QuantStudio 12K Flex (Applied Biosystems), the TaqMan Gene Expression Master Mix (Applied Biosystems), Human ACTB Endogenous Control, pregenomic HBV RNA (forward primer: GGAGTGTGGATTCGCACTCCT; reverse primer: AGATTGAGATCTTCTGCGAC; probe: ACTCCC TCGCCTCGCAGAC), and total HBV RNA (forward primer: CCG TCTGTGCCTTCTCATCTG; reverse primer: AGTCCAAGAGTC CTCTTATGTAAGACCTT; probe: CCGTGTGCACTTCGCTTCA CCTCTGC) TaqMan primer and probe reagents (Life Technologies). The qPCR was performed using the following settings: UDG incubation (2 min; 50°C); enzyme activation (10 min; 95°C); and qPCR (40 cycles with 15 s; 95° for denaturing and 1 min; 60°C for annealing and extension). The relative mRNA expression was analyzed using the comparative cycle threshold (2-ΔΔCt) method normalized to the reference gene, ACTB, and to the no drug control.

Mismatch Analysis of SSO-1/SSO-2

Public HBV complete genome sequences from NCBI have been collected, filtered to patients not taking any medication, and remapped to contain sequences only from genotypes A–H. In total, 3,792 HBV complete genome sequences have been used in the analysis, with 471, 930, 1,310, 633, 203, 202, 19, and 24 sequences for each of the genotypes A–H, respectively.

The target sequence for SSO-2 is aligned, using a local Smith-Waterman algorithm as implemented in R, against all the 3,792 HBV sequences. From the alignment, the number of mismatches, insertions, and/or deletions for each of the HBV complete genome sequences can be found.

AAV-HBV Mouse Model Studies

AAV-HBV was provided by Beijing FivePlus Molecular Medicine Institute (Beijing, China). This recombinant virus carries 1.3 copies of the HBV genome (genotype D; serotype ayw) and is packaged in AAV serotype 8 (AAV8) capsids. C57BL/6 mice were provided by Vital River Laboratories, Beijing, China and SLAC Laboratory Animal, Shanghai, China. Studies were conducted by Covance Pharmaceutical R&D (Shanghai). All procedures in the studies were in compliance with local animal welfare legislation, Covance global policies and procedures, and the Guide for the Care and Use of Laboratory Animals.

C57BL/6 mice (male; 4–6 weeks of age) were injected with 200 μL PBS containing 0.5E12 GE/mL of recombinant virus through the tail vein. Fourteen days after AAV-HBV injection, the mice were bled retro-orbitally to monitor HBsAg and HBV genomic DNA in serum. Based on the HBsAg and HBV DNA levels and body weight, AAV-HBV-infected mice were selected and group randomized (4 animals per group). 5 days later (day 0), animals were dosed subcutaneously by sterile saline or HBV-targeting LNA-oligonucleotides at different dose levels. A total of 4 dosages on days 0, 3, 6, and 9 were followed by two weeks off-treatment monitoring. Serum HBsAg, HBeAg, and HBV DNA were measured twice weekly throughout the study.

Serum HBV DNA was extracted from 50 μL of 1:10 dilution in PBS following the manufacturer's instruction (MagNA Pure 96 DNA Small Volume Kit; Roche).

Real-time qPCR was performed to detect HBV-DNA levels with HBV-specific primers (HBV-F: AAGAAAAACCCCGCCTG TAA; HBV-R: CCTGTTCTGACTACTGCCTCTCC; HBV-probe: 5′+TAMRATAMRA+CCTGATGTGATGTTCTCCATGTTCAGC+ BHQ2-3′; ShangHai Shinegene Molecular Biotechnology). pBR322-HBV GtD ayw 1.3-mer plasmid was used as standard at a different concentration.

Serum HBsAg and HBeAg levels were measured by CLIA (Autobio Diagnostic) as explained above. Serum dilutions of 1:100 for HBeAg and 1:500 for HBsAg in PBS were used to obtain values within the linear range of the standard curve.

Statistical analyses for treatment effect in each group were performed by the Student's t test using GraphPad Prism Software (La Jolla, CA).

Tissue Distribution Studies

C57BL/6 mice were administered with SSO-2 subcutaneously as a single dose of 0.18 and 0.94 μmol/kg (2 animals per dose level and compound). At 48, 96, and 192 hr post-dose, liver and kidney samples were prepared from two animals per time point. Two pieces of 3 × 3 × 3 mm were prepared from each animal and frozen individually in liquid nitrogen. Both kidneys were prepared and frozen in N_2. The liver and kidney samples were subjected to homogenization (Retsch MM300/8 min at 25 Hz) in the presence of proteinase K and incubated overnight at 37°C. The concentration of SSO-1 and SSO-2 in the plasma and tissue samples was determined using hybridization ELISA, as previously described.[52]

In situ hybridization studies were performed by subcutaneous administration of SSO-2 and SSO-1 at 0.18 and 0.94 μmol/kg (3 animals per dose level and compound). After 24 hr, animals were sacrificed and livers were harvested, frozen, and cryosectioned.

Immunohistochemistry and Image Analysis

Two sections separated by approximately 200 μm of formalin-fixed and paraffin-embedded mouse liver were deparaffinized and subjected to heat-induced antigen retrieval in Tris-EDTA glucose (TEG) buffer (pH 9). Following blockage of endogenous peroxidase activity, the sections were blocked in 10% normal serum and incubated with rabbit anti-HBcAg (Dako). The primary antibody was detected and amplified using Brightvision Poly-HRP detection system (Immunologic) and visualized with diaminobenzidine as chromogen.

Finally, sections are counterstained in hematoxylin, coverslipped, and digitized using a 20× objective. Quantitative assessment of HBcAg immunoreactivity was estimated as total counts of positive cellular profiles per area of the liver sections. Profile counting is done by image analysis using Visiomorph (Visiopharm).

Immune Assays

Human whole blood was incubated in round-bottom 96-well plates with test compounds or controls for 6 hr and 45 min at a drug to blood volume ratio of 1:40. After incubation, the plasma was stored at −80°C until required.

ELISA was performed on the samples to measure C3a and C5a (Quidel nos. AO32 and AO25) and interleukin-6 (IL-6), IL-8, tumor necrosis factor alpha (TNF-α), and monocyte chemoattractant protein-1 (MCP1) concentrations (Aushon human arrays nos. 101-261-1-AB and 51-100-1-AB) according to the manufacturer's instructions. Compounds were investigated at 50 μM in triplicates. Assay controls included PBS, zymosan ("alternative pathway," Sigma no. Z4250), heat aggregated immunoglobulin G (IgG) ("classical pathway," Tecomedical no. A114), stop solution ("inhibitor," Tecomedical no. A9576), R848 (InvivoGen no. tlrl-r848), CpG (InvivoGen no. tlrl-2006-1), and poly(dG:dC) (InvivoGen no. tlrl-pgcn).

The stimulation index was calculated relative to PBS-induced values and represented as mean + SD of blood samples originating from 3 donors.

Flow Cytometry Analysis and Western Blot

HepaRG-wild-type (WT) and HepaRG-ASGPR1/2 were differentiated for 4 weeks as described above and harvested using EDTA-Trypsin (Gibco; cat. no. 15050065). The cells were stained with either Purified Mouse IgG1, κ Isotype Control (cat. no. 554121) or Mouse Anti-ASGPR 1 antibody (cat. no. 563655) at matched concentrations. Histograms were derived from gated events based on light-scattering characteristics of viable dHepaRG cells. Flow cytometry was performed on a BD LSRFortessa and analyzed using FlowJo software (Tree Star).

Primary antibodies used for western blot were mouse anti-ASGPR1 (sc-166633; Santa Cruz Biotechnology), mouse anti-ASGPR2 (sc-377113; Santa Cruz), and mouse anti-actin (MAB1501; EMD Millipore). The secondary antibody used was goat anti-mouse-IgG conjugated to alkaline phosphatase (A3562; Sigma). Adherent cells were washed in PBS and then lysed in the culture flask with ice-cold radioimmunoprecipitation assay (RIPA) lysis buffer (Rockland MB-030-0050) and cleared at 14,000 *g* for 5 min. Supernatants of protein extracts were heated in SDS buffer containing reducing reagent (NP0007 and NP0009; Thermo Fisher Scientific) at 70°C for 10 min before loading on 4%–12% polyacrylamide gels (NP0321; Invitrogen) with 2-(N-morpholino)ethanesulfonic acid (MES) running buffer. Proteins were transferred to nitrocellulose membrane using the iBlot transfer system (Invitrogen) for 7 min. Membranes were blocked with 5% BSA in Tris-buffered saline tween (TBST) buffer for 1 hr before incubation with primary antibody at 4°C for overnight. Membranes were washed three times with TBST buffer before incubation with secondary antibody for 1 hr at 4°C. After three times washing with TBST buffer, signal was revealed by the NTB/BCIP staining solution (11697471001; Roche Life Science).

SUPPLEMENTAL INFORMATION

Supplemental Information includes three figures and can be found with this article online at https://doi.org/10.1016/j.omtn.2018.02.005.

AUTHOR CONTRIBUTIONS

H.J., J.A.T.Y., and S.O. initiated and supervised the studies. H.J., N.A., X.Z., J.B., J.W., H.M., R.P., J.R., C.P., M.J., T.S., L.P., A.L., T.P., and W.D. designed and performed experiments or contributed to data analysis. H.J., H.M., R.P., S.O., and J.A.T.Y. wrote the manuscript.

CONFLICTS OF INTEREST

H.J., H.M., J.W., X.Z., A.L., T.P., J.B., L.P., N.A., M.J., T.S., C.P., W.D., R.P., J.R., J.A.T.Y., and S.O. are or have been employees of Hoffman-LaRoche. No conflicts of interest are declared.

ACKNOWLEDGMENTS

The funding for this study was provided through Hoffman-LaRoche internal funds.

SUPPORTING CITATIONS

The following reference appears in the Supplemental Information: Hagedorn et al.[53]

REFERENCES

1. Sunbul, M. (2014). Hepatitis B virus genotypes: global distribution and clinical importance. World J. Gastroenterol. *20*, 5427–5434.
2. WHO (2017). Global Hepatitis Report, 2017 (World Health Organization).
3. Chisari, F.V., Isogawa, M., and Wieland, S.F. (2010). Pathogenesis of hepatitis B virus infection. Pathol. Biol. (Paris) *58*, 258–266.
4. Chan, S.L., Wong, V.W., Qin, S., and Chan, H.L. (2016). Infection and cancer: the case of hepatitis B. J. Clin. Oncol. *34*, 83–90.
5. Zoulim, F., and Durantel, D. (2015). Antiviral therapies and prospects for a cure of chronic hepatitis B. Cold Spring Harb. Perspect. Med. *5*, a021501.
6. Ferrari, C. (2015). HBV and the immune response. Liver Int. *35* (*Suppl 1*), 121–128.
7. Quasdorff, M., and Protzer, U. (2010). Control of hepatitis B virus at the level of transcription. J. Viral Hepat. *17*, 527–536.
8. Levrero, M., Pollicino, T., Petersen, J., Belloni, L., Raimondo, G., and Dandri, M. (2009). Control of cccDNA function in hepatitis B virus infection. J. Hepatol. *51*, 581–592.
9. Kennedy, P.T.F., Litwin, S., Dolman, G.E., Bertoletti, A., and Mason, W.S. (2017). Immune tolerant chronic hepatitis B: the unrecognized risks. Viruses *9*, E96.
10. Frebel, H., Richter, K., and Oxenius, A. (2010). How chronic viral infections impact on antigen-specific T-cell responses. Eur. J. Immunol. *40*, 654–663.
11. Ochel, A., Cebula, M., Riehn, M., Hillebrand, U., Lipps, C., Schirmbeck, R., Hauser, H., and Wirth, D. (2016). Effective intrahepatic CD8+ T-cell immune responses are induced by low but not high numbers of antigen-expressing hepatocytes. Cell. Mol. Immunol. *13*, 805–815.
12. Kondo, Y., Ninomiya, M., Kakazu, E., Kimura, O., and Shimosegawa, T. (2013). Hepatitis B surface antigen could contribute to the immunopathogenesis of hepatitis B virus infection. ISRN Gastroenterol. *2013*, 935295.

13. Woltman, A.M., Op den Brouw, M.L., Biesta, P.J., Shi, C.C., and Janssen, H.L. (2011). Hepatitis B virus lacks immune activating capacity, but actively inhibits plasmacytoid dendritic cell function. PLoS ONE *6*, e15324.

14. Op den Brouw, M.L., Binda, R.S., van Roosmalen, M.H., Protzer, U., Janssen, H.L., van der Molen, R.G., and Woltman, A.M. (2009). Hepatitis B virus surface antigen impairs myeloid dendritic cell function: a possible immune escape mechanism of hepatitis B virus. Immunology *126*, 280–289.

15. Chen, Y., Wei, H., Sun, R., and Tian, Z. (2005). Impaired function of hepatic natural killer cells from murine chronic HBsAg carriers. Int. Immunopharmacol. *5*, 1839–1852.

16. Vanwolleghem, T., and Boonstra, A. (2017). Focus on the liver: host-virus interactions in HBV. J. Hepatol. *66*, 884–885.

17. Lebossé, F., Testoni, B., Fresquet, J., Facchetti, F., Galmozzi, E., Fournier, M., Hervieu, V., Berthillon, P., Berby, F., Bordes, I., et al. (2017). Intrahepatic innate immune response pathways are downregulated in untreated chronic hepatitis B. J. Hepatol. *66*, 897–909.

18. Viney, N.J., van Capelleveen, J.C., Geary, R.S., Xia, S., Tami, J.A., Yu, R.Z., Marcovina, S.M., Hughes, S.G., Graham, M.J., Crooke, R.M., et al. (2016). Antisense oligonucleotides targeting apolipoprotein(a) in people with raised lipoprotein(a): two randomised, double-blind, placebo-controlled, dose-ranging trials. Lancet *388*, 2239–2253.

19. Janssen, H.L., Kauppinen, S., and Hodges, M.R. (2013). HCV infection and miravirsen. N. Engl. J. Med. *369*, 878.

20. Schluep, T., Lickliter, J., Hamilton, J., Lewis, D.L., Lai, C.L., Lau, J.Y., Locarnini, S.A., Gish, R.G., and Given, B.D. (2016). Safety, tolerability and pharmacokinetics of ARC-520 injection, an RNA interference-based therapeutic for the treatment of chronic hepatitis B virus infection, in healthy volunteers. Clin. Pharmacol. Drug Dev. *6*, 350–362.

21. Rosenbohm, C., Pedersen, D.S., Frieden, M., Jensen, F.R., Arent, S., Larsen, S., and Koch, T. (2004). LNA guanine and 2,6-diaminopurine. Synthesis, characterization and hybridization properties of LNA 2,6-diaminopurine containing oligonucleotides. Bioorg. Med. Chem. *12*, 2385–2396.

22. van Poelgeest, E.P., Hodges, M.R., Moerland, M., Tessier, Y., Levin, A.A., Persson, R., Lindholm, M.W., Dumong Erichsen, K., Ørum, H., Cohen, A.F., and Burggraaf, J. (2015). Antisense-mediated reduction of proprotein convertase subtilisin/kexin type 9 (PCSK9): a first-in-human randomized, placebo-controlled trial. Br. J. Clin. Pharmacol. *80*, 1350–1361.

23. Moisan, A., Gubler, M., Zhang, J.D., Tessier, Y., Dumong Erichsen, K., Sewing, S., Gérard, R., Avignon, B., Huber, S., Benmansour, F., et al. (2017). Inhibition of EGF uptake by nephrotoxic antisense drugs in vitro and implications for preclinical safety profiling. Mol. Ther. Nucleic Acids *6*, 89–105.

24. Prakash, T.P., Graham, M.J., Yu, J., Carty, R., Low, A., Chappell, A., Schmidt, K., Zhao, C., Aghajan, M., Murray, H.F., et al. (2014). Targeted delivery of antisense oligonucleotides to hepatocytes using triantennary N-acetyl galactosamine improves potency 10-fold in mice. Nucleic Acids Res. *42*, 8796–8807.

25. Fitzgerald, K., White, S., Borodovsky, A., Bettencourt, B.R., Strahs, A., Clausen, V., Wijngaard, P., Horton, J.D., Taubel, J., Brooks, A., et al. (2017). A highly durable RNAi therapeutic inhibitor of PCSK9. N. Engl. J. Med. *376*, 41–51.

26. Yu, R.Z., Graham, M.J., Post, N., Riney, S., Zanardi, T., Hall, S., Burkey, J., Shemesh, C.S., Prakash, T.P., Seth, P.P., et al. (2016). Disposition and pharmacology of a GalNAc3-conjugated ASO targeting human lipoprotein (a) in mice. Mol. Ther. Nucleic Acids *5*, e317.

27. Wooddell, C.I., Yuen, M.F., Chan, H.L., Gish, R.G., Locarnini, S.A., Chavez, D., Ferrari, C., Given, B.D., Hamilton, J., Kanner, S.B., et al. (2017). RNAi-based treatment of chronically infected patients and chimpanzees reveals that integrated hepatitis B virus DNA is a source of HBsAg. Sci. Transl. Med. *9*, eaan0241.

28. Wooddell, C.I., Rozema, D.B., Hossbach, M., John, M., Hamilton, H.L., Chu, Q., Hegge, J.O., Klein, J.J., Wakefield, D.H., Oropeza, C.E., et al. (2013). Hepatocyte-targeted RNAi therapeutics for the treatment of chronic hepatitis B virus infection. Mol. Ther. *21*, 973–985.

29. Arrowhead (2016). Press Release: clinical update call. http://ir.arrowheadpharma.com/static-files/0e6e50dc-5d2b-43cb-a531-2c737be21043.

30. Billioud, G., Kruse, R.L., Carrillo, M., Whitten-Bauer, C., Gao, D., Kim, A., Chen, L., McCaleb, M.L., Crosby, J.R., Hamatake, R., et al. (2016). In vivo reduction of hepatitis B virus antigenemia and viremia by antisense oligonucleotides. J. Hepatol. *64*, 781–789.

31. Stein, C.A., Hansen, J.B., Lai, J., Wu, S., Voskresenskiy, A., Høg, A., Worm, J., Hedtjärn, M., Souleimanian, N., Miller, P., et al. (2010). Efficient gene silencing by delivery of locked nucleic acid antisense oligonucleotides, unassisted by transfection reagents. Nucleic Acids Res. *38*, e3.

32. Rajeev, K.G., Nair, J.K., Jayaraman, M., Charisse, K., Taneja, N., O'Shea, J., Willoughby, J.L., Yucius, K., Nguyen, T., Shulga-Morskaya, S., et al. (2015). Hepatocyte-specific delivery of siRNAs conjugated to novel non-nucleosidic trivalent N-acetylgalactosamine elicits robust gene silencing in vivo. ChemBioChem *16*, 903–908.

33. Gripon, P., Rumin, S., Urban, S., Le Seyec, J., Glaise, D., Cannie, I., Guyomard, C., Lucas, J., Trepo, C., and Guguen-Guillouzo, C. (2002). Infection of a human hepatoma cell line by hepatitis B virus. Proc. Natl. Acad. Sci. USA *99*, 15655–15660.

34. Dion, S., Bourgine, M., Godon, O., Levillayer, F., and Michel, M.L. (2013). Adeno-associated virus-mediated gene transfer leads to persistent hepatitis B virus replication in mice expressing HLA-A2 and HLA-DR1 molecules. J. Virol. *87*, 5554–5563.

35. Encyclopædia Britannica. (2009). Leaf-nosed bat. Encyclopædia Britannica, https://www.britannica.com/animal/leaf-nosed-bat.

36. Bon, C., Hofer, T., Bousquet-Mélou, A., Davies, M.R., and Krippendorff, B.F. (2017). Capacity limits of asialoglycoprotein receptor-mediated liver targeting. MAbs *9*, 1360–1369.

37. Wu, J., and Chen, Z.J. (2014). Innate immune sensing and signaling of cytosolic nucleic acids. Annu. Rev. Immunol. *32*, 461–488.

38. Kawasaki, T., Kawai, T., and Akira, S. (2011). Recognition of nucleic acids by pattern-recognition receptors and its relevance in autoimmunity. Immunol. Rev. *243*, 61–73.

39. Lucifora, J., Salvetti, A., Marniquet, X., Mailly, L., Testoni, B., Fusil, F., Inchauspé, A., Michelet, M., Michel, M.L., Levrero, M., et al. (2017). Detection of the hepatitis B virus (HBV) covalently-closed-circular DNA (cccDNA) in mice transduced with a recombinant AAV-HBV vector. Antiviral Res. *145*, 14–19.

40. Wang, H., and Ryu, W.S. (2010). Hepatitis B virus polymerase blocks pattern recognition receptor signaling via interaction with DDX3: implications for immune evasion. PLoS Pathog. *6*, e1000986.

41. Lan, S., Wu, L., Wang, X., Wu, J., Lin, X., Wu, W., and Huang, Z. (2016). Impact of HBeAg on the maturation and function of dendritic cells. Int. J. Infect. Dis. *46*, 42–48.

42. Kumar, M., Jung, S.Y., Hodgson, A.J., Madden, C.R., Qin, J., and Slagle, B.L. (2011). Hepatitis B virus regulatory HBx protein binds to adaptor protein IPS-1 and inhibits the activation of beta interferon. J. Virol. *85*, 987–995.

43. D'Souza, A.A., and Devarajan, P.V. (2015). Asialoglycoprotein receptor mediated hepatocyte targeting - strategies and applications. J. Control. Release *203*, 126–139.

44. Li, Y., Huang, G., Diakur, J., and Wiebe, L.I. (2008). Targeted delivery of macromolecular drugs: asialoglycoprotein receptor (ASGPR) expression by selected hepatoma cell lines used in antiviral drug development. Curr. Drug Deliv. *5*, 299–302.

45. Durantel, D., and Zoulim, F. (2016). New antiviral targets for innovative treatment concepts for hepatitis B virus and hepatitis delta virus. J. Hepatol. *64* (1, Suppl), S117–S131.

46. Werle-Lapostolle, B., Bowden, S., Locarnini, S., Wursthorn, K., Petersen, J., Lau, G., Trepo, C., Marcellin, P., Goodman, Z., Delaney, W.E., 4th, et al. (2004). Persistence of cccDNA during the natural history of chronic hepatitis B and decline during adefovir dipivoxil therapy. Gastroenterology *126*, 1750–1758.

47. Isogawa, M., Chung, J., Murata, Y., Kakimi, K., and Chisari, F.V. (2013). CD40 activation rescues antiviral $CD8^+$ T cells from PD-1-mediated exhaustion. PLoS Pathog. *9*, e1003490.

48. Huang, Y. (2017). Preclinical and clinical advances of GalNAc-decorated nucleic acid therapeutics. Mol. Ther. Nucleic Acids *6*, 116–132.

49. Alnylam (2017). Press release: Alnylam and Vir form strategic alliance to advance RNAi therapeutics for infectious diseases. http://investors.alnylam.com/node/21911/pdf.

50. Janssen, H.L., Reesink, H.W., Lawitz, E.J., Zeuzem, S., Rodriguez-Torres, M., Patel, K., van der Meer, A.J., Patick, A.K., Chen, A., Zhou, Y., et al. (2013). Treatment of HCV infection by targeting microRNA. N. Engl. J. Med. *368*, 1685–1694.

51. Lill, J., and Trussardi, R. (2017). Processes for the Preparation of Galnac Acid Derivatives (Google Patents).

52. Hildebrandt-Eriksen, E.S., Aarup, V., Persson, R., Hansen, H.F., Munk, M.E., and Ørum, H. (2012). A locked nucleic acid oligonucleotide targeting microRNA 122 is well-tolerated in cynomolgus monkeys. Nucleic Acid Ther. *22*, 152–161.

53. Hagedorn, P.H., Yakimov, V., Ottosen, S., Kammler, S., Nielsen, N.F., Høg, A.M., Hedtjärn, M., Meldgaard, M., Møller, M.R., Orum, H., et al. (2013). Hepatotoxic potential of therapeutic oligonucleotides can be predicted from their sequence and modification pattern. Nucleic Acid Ther. *23*, 302–310.